

Vitamin C Binds to SARS Coronavirus-2 Main Protease Essential for Viral Replication

Tek Narsingh Malla^{1&}, Suraj Pandey^{1&}, Luis Aldama², Dennisse Feliz^{2,3}, Moraima Noda², Ishwor Poudyal¹, George N. Phillips Jr.⁴, Emina A. Stojković^{2*}, Marius Schmidt^{1*}

¹Department of Physics, University of Wisconsin Milwaukee, Milwaukee, WI 53211 USA

²Department of Biology, Northeastern Illinois University, Chicago, IL 60625 USA

³Department of Chemistry, Northeastern Illinois University, Chicago, IL 60625 USA

⁴Department of BioSciences, Rice University, Houston, TX 77005 USA

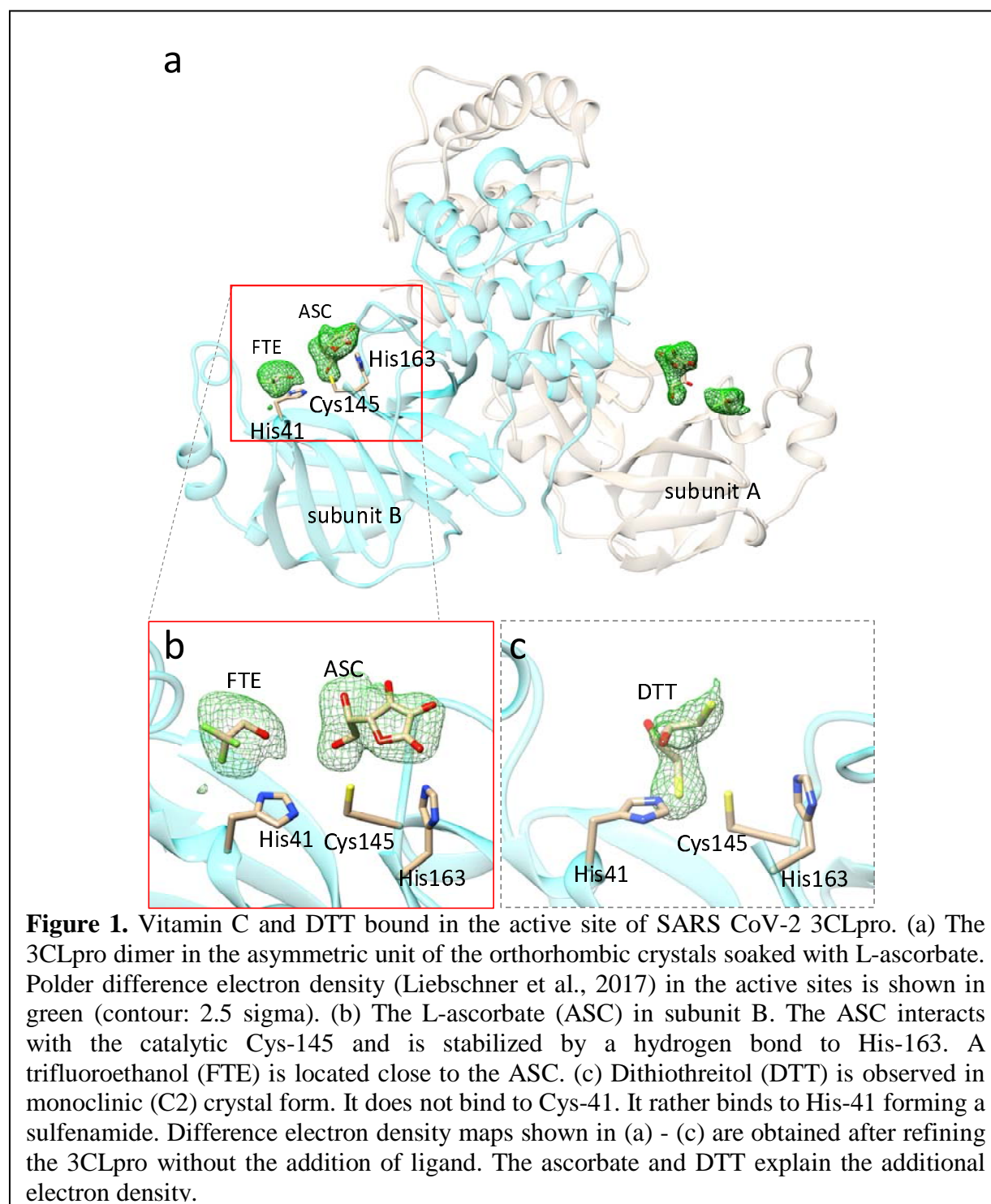
[&]contributed equally

^{*}corresponding authors

Abstract

There is an urgent need for anti-viral agents that treat and/or prevent Covid-19 caused by SARS-Coronavirus (CoV-2) infections. The replication of the SARS CoV-2 is dependent on the activity of two cysteine proteases, a papain-like protease, PL-pro, and the 3C-like protease known as main protease Mpro or 3CLpro. The shortest and the safest path to clinical use is the repurposing of drugs with binding affinity to PLpro or 3CLpro that have an established safety profile in humans. Several studies have reported crystal structures of SARS-CoV-2 main protease in complex with FDA approved drugs such as those used in treatment of hepatitis C. Here, we report the crystal structure of 3CLpro in complex Vitamin C (L-ascorbate) bound to the protein's active site at 2.5 Ångstrom resolution. The crystal structure of the Vitamin C 3CLpro complex may aid future studies on the effect of Vitamin C not only on the coronavirus main protease but on related proteases of other infectious viruses.

29



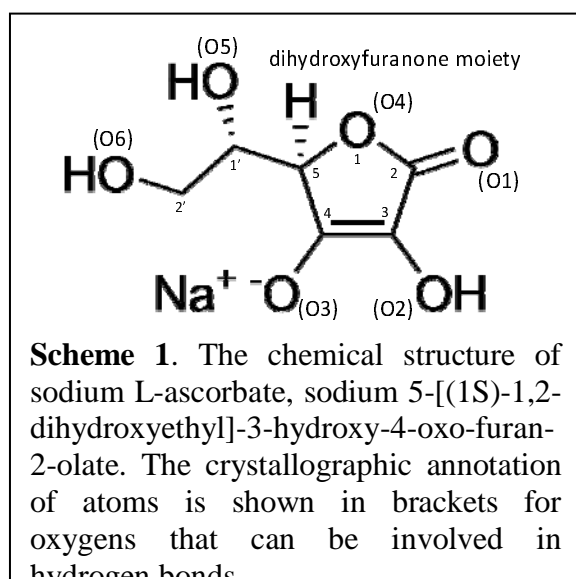
30 The Covid-19 pandemic, caused by a novel severe acute respiratory syndrome (SARS)
 31 coronavirus 2, has paralyzed public life globally. It has resulted in excess of 500,000 deaths in
 32 the US alone as of April 2021. Although potent vaccines are now available, they are optional, not

tested in children and potentially not as effective against new viral mutant variants emerging world-wide (LITER). The need for an effective inexpensive treatment and prevention of Covid-19 still exists as large number of infections with potentially severe or lethal outcomes are still reported daily. SARS CoV-2 is a large, enveloped single-stranded RNA betacoronavirus (Cui et al., 2019). The viral RNA encodes two open reading frames that, generates two polyproteins pp1a and pp1ab8. The polyproteins are processed by two viral cysteine proteases: a papain-like protease (PLpro) and a 3C-like protease, also referred to as the main protease (Mpro) or 3CLpro, that cleave multiple sites to release non-structural proteins (nsp1-16). These non-structural proteins form the replicase complex responsible for replication and transcription of the viral genome and have led to 3CLpro and PLpro being the primary targets for antiviral drug development. The 3CLpro is a chymotrypsin-like cysteine protease with a Cys/His dyad in the active site (Fig. 1a). The 3C refers to region 3C in the genome of the *picornaviridae* family, where a similar protease is found (Ramajayam et al., 2011). In coronaviruses, the 3CLpro is located in the non-structural protein (NSP) 5 coding region of the virus RNA genome (Wu et al., 2020).

High throughput structure based drug discovery experiments on 3CL-pro were recently conducted by large groups of scientists at synchrotrons such as Petra III (Gunther et al., 2021), Diamond (Douangamath et al., 2020) and NSLS-II (to be published) among others. This approach was also rapidly deployed after the 2002 SARS-CoV-1 outbreak, with earlier work by the Hilgenfeld group on Mpro (3CLpro) of coronarviruses leading to crystal structures of SARS-CoV-2 Mpro and inhibitor complexes (Zhang, Lin, Kusov, et al., 2020; Zhang, Lin, Sun, et al., 2020). Active sites of coronavirus Mpro are well conserved and those of enteroviruses (3Cpro) are functionally similar: thus, providing an excellent opportunity to develop broad-spectrum antivirals with structural biology approach. However, the most inhibitors investigated so far are marginally water soluble. They have to be added to the crystals in an organic solvent, or they can be co-crystallized. Their relative scarcity, potential toxicity and unspecificity, and a potentially expensive price tag prevents their wide-spread use. Inexpensive, water soluble, and readily available drugs to combat Covid-19 are urgently required.

Vitamin C has been shown to have antiviral activity for more than half a century, including work of the two-times Nobel Laureate Linus Pauling (Pauling, 1970). Vitamin C is a six-carbon compound (Scheme 1) and a potent antioxidant. It is available in synthetic form and found naturally in Indian gooseberry, citrus fruits and green leafy vegetables. The revival of interest in Vitamin C therapy for acute inflammatory disorders, grounded in sound biological rationale, follows decades of research. Emerging literature suggests that Vitamin C may also play an adjunctive role in the treatment of a variety of viral infections (Colunga Biancatelli et al., 2020; Fowler Iii et al., 2017). A number of observers including Linus Pauling have suggested in the past that Vitamin C in high dosages is directly virucidal (Furuya et al., 2008; Harakeh et al., 1990; Klein, 1945; Pauling, 1970). This assumption was based on in vitro studies, where very high doses of Vitamin C, in the presence of free copper and/or iron, has virucidal activity, presumably through the generation of hydrogen peroxide and other radical species (Furuya et al., 2008; Klein, 1945).

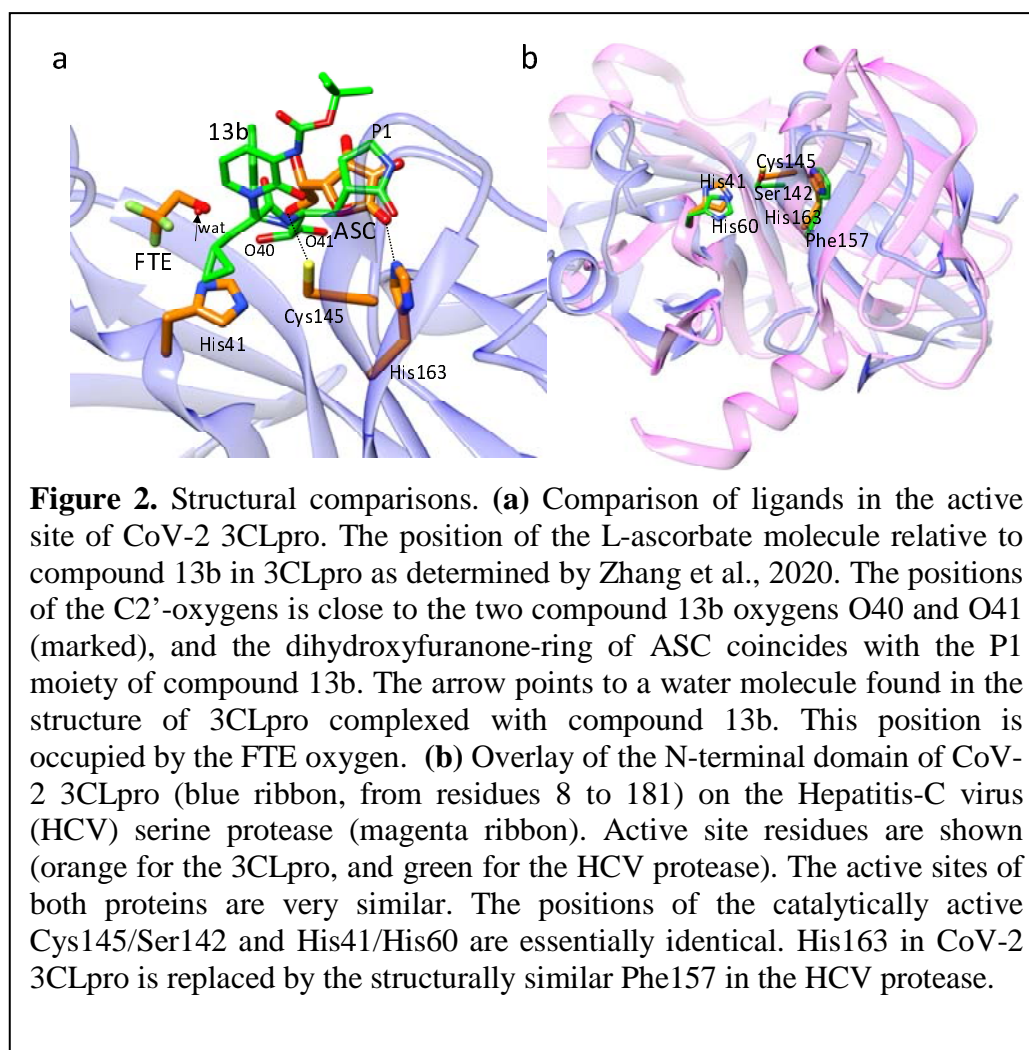
76



A recent clinical study of injecting high doses of vitamin-C (> 20 g) intravenously to combat Covid-19 yielded promising results (Zhao et al., 2021). In another study 8 g of Vitamin C was administered orally over three meals together with zinc (Thomas et al., 2021). The results were inconclusive although a positive trend is apparent. So far, it could not be demonstrated that Vitamin C is directly virucidal against Covid-19 *in vivo*.

In order to investigate the binding of Vitamin-C directly to the CoV-2 3CLpro, we co-crystallized CoV-2 3CLpro with low concentrations (5 mmol/L) of L-ascorbate and soaked these crystals before freezing for 3 min in 120 mmol/L ascorbate (Supplementary Material). Difference electron density that can be assigned to ascorbate appears in the active sites near Cys-145 and His-163 of both subunits (Fig. 1). The L-ascorbates only weakly interact with Cys-145 (between 3 Å and 3.7 Å to the sulfur, Tab. 1) but form a tight hydrogen bonding network with Asn-142, Gly-143(N), His-163 and Gln-166 (Fig.

94 S1 and Tab. 1). In addition to the L-ascorbate electron density, an additional density feature is
 95 present in the active site. The pillow-like electron density (Fig. 1 b) is interpreted with a
 96 trifluoroethanol (FTE) that has been provided as an additive to the crystallization buffer. The
 97 interaction of the FTE with the nearby L-ascorbate is weak as the closest distance is larger than 4
 98 Å (Tab. 1). Fig. 2 compares the L-ascorbate position to the position of compound 13b in the
 99 active site of the 3CLpro. Compound 13b is a potent inhibitor of the 3CLpro (Zhang, Lin, Kusov,
 100 et al., 2020). The positions of the two compound 13b oxygens O40 and O41 in the 3CLpro are
 101 close to the C2' oxygen of the ascorbate (Fig. 2 a). The dihydroxyfuranone ring (Scheme 1) of
 102 the ascorbate occupies a similar position as the moiety P1 of compound 13b (Fig. 2 a). The FTE
 103 oxygen position is reflected by a structural water found in the compound 13b complexed 3CLpro
 104 structure. 3CLpro can also be crystallized in the presence of dithiotreitol (DTT) (Zhang, Lin,
 105 Sun, et al., 2020). DTT binds with one of its sulfurs between the Cys-145 and His-41 (Fig. 1 c).
 106 As the distance to the His-41 N_e is substantially shorter (1.5 Å) than the one to the Cys-145
 107 sulfur (2.3 Å), the DTT forms a sufenamide with His-41 which is a critical amino acid for the
 108 catalytic mechanism of the 3CLpro.



109

110 A search for ascorbate in the protein data bank yields 645 protein structures with only 40

111 structures that have a bound ascorbate. None of the 40 structures are viral proteins. To our

112 knowledge, this is the first structure of a viral protein with ascorbate bound in the active site. The

113 CoV-2 3CLpro has homologues in many other viruses different from coronavirus. As mentioned

114 above, a similar (3C) protease can be found in picornaviruses (Ramajayam et al., 2011).

115 Members of the *picornaviridae* family cause diseases such as polio (poliovirus),

116 encephalomyelitis (encephalomyocarditis virus) and the common cold (rhinovirus) (Sharma &

117 Gupta, 2017). Moreover, the structure of the N-terminal domain of the CoV-2 3CLpro, as well as

118 that of its active site is very similar to the structure of the hepatitis-C virus (HCV) protease (Fig.

119 2), except that the HCV protease is a serine protease. However, even the HCV protease Ser-142

oxygen position is essentially identical to that of the Cys-145 sulfur in the 3CLpro. The binding of Vitamin C to the CoV-2 3CLpro might point to reasons why Vitamin C could be beneficial for the treatment of coronavirus caused diseases such as SARS and middle east respiratory syndrome (MERS) who have structurally similar 3CLpros (Hilgenfeld, 2014; Zhang, Lin, Sun, et al., 2020). Moreover, Vitamin C might also bind to proteases of other viruses, and assists in the treatment of diseases mentioned above and others such as AIDS (Harakeh et al., 1990), herpes (Furuya et al., 2008; Hoog et al., 1997), rhinovirus induced respiratory distress syndrome (Fowler Iii et al., 2017) and even rabies (Banic, 1975).

The available inhibition test (the ‘Untagged (SARS-CoV-2) Assay Kit’, BPS Biosciences) cannot be used to determine an inhibitory effect of L-ascorbate as the ascorbate quenches the fluorescence of the enzymatically produced product at higher concentrations and inhibition tests are inconclusive. Since ascorbate is detected in the crystal structure, it may well be that inhibition of proteases with Vitamin C, or perhaps with one of its derivatives (Mescic Macan et al., 2019) that may even bind directly to the catalytically important Cys-145, becomes an important factor in the treatment of Covid-19 cases and maybe other virus caused infections (Colunga Biancatelli et al., 2020). Further investigations are necessary.

Table 1. Comparison ligand interactions with conserved amino acids in the active site of subunits A and B. Designated atoms of amino acids in subunits A and B and ascorbate ligands that interact are labelled according to annotations in the refined structure (see also Scheme 1).

3CLpro / Ascorbate		
	Distances [Å] Subunit A	Distances [Å] Subunit B
Asn142-NOD2 / O5	2.4	2.4
Asn 142-NOD2 / O3	3.2	2.6
Cys145-SG / O6	3.0	3.1
Cys145-SG/ O4	3.7	3.4
His163-NE2 / O1	3.3	2.4
His 163-NE2/O4	3.7	3.9
Glu166-OE2 / O2	3.0	3.0
Gly143-N / O6	2.9	3.1
3CLpro / Trifluoroethanol (FTE)		
His41-ND / F*	3.0	2.9
His41-O / F*	2.8	3.2
CYS44-O / F*	3.0	2.9
Ser 46-OG / O	3.2	4.9
ASC-O6 / O**	4.7	4.6
3CLpro / Dithiothreitol (DTT)		
His41-NE2 / S4	1.4	n.a.***
Cys145-SG / S4	2.6	---
H ₂ O111-O / S1	2.6	---

*shortest to any of the three fluor atoms
 ** shortest FTE to Ascorbate distance
 ***only one subunit in the asymmetric unit

Supplementary Material

Expression. The CoV-2 3CLpro sequence was synthesized (GenScript) for optimized expression in *E. coli* according to sequence information published previously (Zhang, Lin, Sun, et al., 2020). In short, the N-terminus of 3CLpro is fused to glutathione-S-transferase (GST). It further has a 6-His tag at the c-terminus. The N-terminal GST will be autocatalytically cleaved off after expression due to an engineered 3CLpro cleavage sequence. Although the His tag can be cleaved off by a PreScission protease, the tag did not interfere with crystallization and consequently was left on. Overexpression and protein purification protocols were modified from previous reports. *E. coli* were grown to 0.8 OD₆₀₀ at 37° in terrific broth. Expression was induced by 1 mmol/L IPTG at 25° C. After 3 h of expression, the culture was induced a second time (1 mmol/L IPTG), and shaken overnight at 20° C. The yield is about 80 mg for a 6 L culture. Cells were resuspended in lysis buffer (20mM Tris Base, 150 mmol/L NaCl, pH 7.8.). After lysis of the bacterial cells, debris was centrifuged at 50,000 g for 1 hour. The lysate was let stand at room temperature for 3 h (overnight is also possible). After this, the lysate was pumped through a column containing 15 mL of Talon Cobalt resin (TAKARA). The resin was washed without using imidazole using a wash cycle consisting of low salt (20 mmol/L Tris Base, 50 mmol/L NaCl, pH 7.8), high salt (20 mmol/L Tris Base, 1 mol/L NaCl, pH 7.8) and low salt (as above) solutions (about 20 column volumes each). After the wash cycle was completed, the column was let stand for an additional 2 h at room temperature followed by another wash cycle. The final product was eluted by 300 mmol/L imidazole. Buffer exchange was achieved at 4 ° C by either by 3 times spin-concentration and re-dilution with 20 mmol/L Tris base, 150 mmol/L NaCl, 25 mmol/L Na-ascorbate, or by dialyzing immediately in 20 mmol/L Tris base, 150 mmol/L NaCl, 0.1 mmol/L dithiotreitol (DTT), pH 7.8. The preparations were concentrated to a 3CLpro concentration of 20 mg/mL. Since the 6-His tag was not cleaved off, this one step purification protocol required only ~10 h from cell lysis to the pure 3CLpro product. The product is within 1.7 Da of the theoretical molecular weight as determined by mass spectroscopy.

Crystallization. The concentrated 3CLpro containing DTT was diluted to 4 mg/mL. 100 µL of the diluted 3CLpro was mixed (1:1) in batch mode with the same amount of 25 % PEG 3350, Bis-Tris 100 mmol/L, pH 6.5. Rectangular shaped crystals with dimensions of about 200 x 30 x

30 μm^3 were obtained. Crystals of the ascorbate containing 3CLpro were obtained by the hanging drop method by mixing 2 μL of 30 mg/mL protease with an equal amount of a reservoir solution containing 15 % PEG 3350, 5 mmol/L ascorbate, and trifluoroethanol (FTE) (4 %) as an additive. Crystals formed long thin needles after 3-day incubation at 16° C. Crystals were soaked in mother liquor containing an addition of 120 mmol/L ascorbate and 20 % glycerol as a cryoprotectant for 3 min before freezing.

Data Collection and Structure determination. The crystals were mounted in Mitegen micro-loops (30 - 50 μm) and directly frozen in pucks suspended in liquid nitrogen for automated (robotic) data collection. The dewar with the pucks were provided to the Advanced Photon Source, Argonne National Lab, Lemont, IL, for robotic data collection at Sector-19 (Structural Biology Center, SBC, beamline 19-ID-D). Data collection was fully remote due to restriction of the COVID-19 pandemic. Dataset to 2.2 Å and 2.5 Å, respectively, were collected (0.5° rotation and 0.8 s exposure per detector readout for a total of 180°) on the 3CLpro with DTT and L-ascorbate, respectively. Data was processed with HKL3000 (Minor et al., 2006). Data statistics in shown in Tab. 1. The spacegroup of the DTT containing crystals was C2. For refinement, the 3CLpro structure with pdb access code 6Y2E (Zhang, Lin, Sun, et al., 2020) was used as initial model. Molecular replacement was not necessary as the model fits immediately. Refinement was achieved using refmac (Murshudov et al., 2011) (version 5.8.0238). The electron density of the DTT becomes apparent by a difference electron density feature in between His-41 and Cys-145 (Fig. 1 c). With L-ascorbate and FTE in the buffer, the spacegroup becomes P2₁2₁2₁ with cell constants not found so far for the CoV-2 3CLpro. Molecular replacement was performed by Phaser (Oeffner et al., 2013) version 2.8.2 using pdb-entry 6XQT (Kneller et al., 2020) as a search model. After refinement of the molecular replacement solution, difference electron density of both, the L-ascorbate and the FTE becomes apparent in the active sites of both subunits (Fig. 1 a). The positions and orientations of the L-ascorbates and the FTE molecules were determined with the help of Polder maps (Fig. 1a and b) (Liebschner et al., 2017) calculated using Phenix (Adams et al., 2010) v1.19.2-4158. After conventional refinement in Phenix, grouped occupancy refinement resulted in sub-stoichiometric concentrations with occupancy values of the L-ascorbates varying from ~60 % in subunit A to ~70 % in subunit B.

210 **Table S1.** Data collection and refinement statistics.

	SARS CoV-2 3CLpro	
Beamline	APS 19-ID-D	
Temperature	110 K	
Ligand	L-ascorbate (Vitamin C)	Dithiothreitol (DTT)
Resolution (Å)	2.3	2.3
Space group	P2 ₁ 2 ₁ 2 ₁	C2
Unit-cell parameters (Å, °)	a = 65.4 Å b = 67.5 Å c = 157.5 Å α=90° β=90° γ=90°	a = 113.39 Å b = 53.4 Å c = 44.7 Å α=90° β=102.8° γ=90°
No of unique reflections	30845	9426
Redundancy	5.7 (3.9)	3.1 (1.8)
Completeness (%)	98.2 (90.0)	70.0
CC1/2 @ dmin	45.2	47.6
R _{merge} (%)	20.4 (145.6)	7.3 (122)
Model Building/ Refinement	Phenix 1.19.2-4158 to 2.3 Å	refmac 5.8.0258 to 2.2 Å
R _{cryst} /R _{free} (%)	21.0/24.4	19.1/26.3
# subunit/asymmetric unit	2	1
# residues/subunit	303/310*	303
additional ligand	trifluoroethanol (FTE)	n.o.
ligand occupancy	Vitamin C: A 0.66; B 0.67** FTE: A 0.66; B: 0.68	0.85
# water	198	1184
R.m.s.d. bonds (Å)/angles (°)	0.005/1.07	0.007/0.949
Coordinate Error (Å)	0.25	0.18

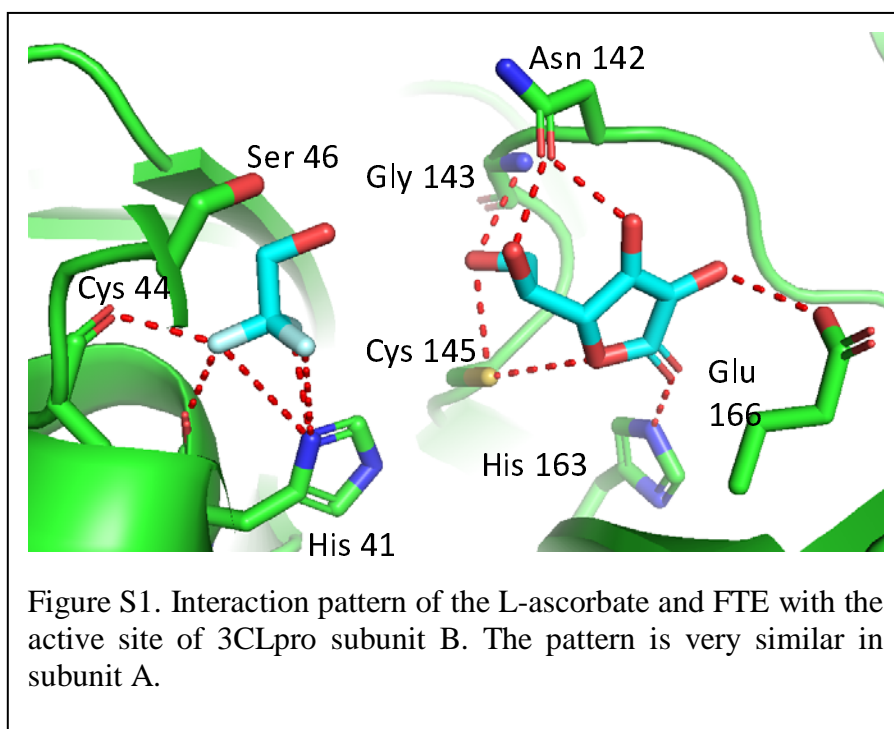
211 *in subunit B, electron density for seven additional C-terminal residues including that of two
212 histidines of the hexa-his tag can be observed.

213 **the difference electron density in any F^{obs}-F^{calc} difference map including the Polder map is
214 visually weaker in the active site of subunit A compared to that of subunit B.

215 n.o.: no additional ligand

216

217
218



References

- Adams, P. D., Afonine, P. V., Bunkoczi, G., Chen, V. B., Davis, I. W., Echols, N., Headd, J. J., Hung, L. W., Kapral, G. J., Grosse-Kunstleve, R. W., McCoy, A. J., Moriarty, N. W., Oeffner, R., Read, R. J., Richardson, D. C., Richardson, J. S., Terwilliger, T. C., & Zwart, P. H. (2010). PHENIX: a comprehensive Python-based system for macromolecular structure solution. *Acta Crystallogr D Biol Crystallogr*, 66(Pt 2), 213-221. <https://doi.org/10.1107/S0907444909052925>
- Banic, S. (1975). Prevention of Rabies by Vitamin C. *Nature*, 258, 2.
- Colunga Biancatelli, R. M. L., Berrill, M., & Marik, P. E. (2020). The antiviral properties of vitamin C. *Expert Rev Anti Infect Ther*, 18(2), 99-101. <https://doi.org/10.1080/14787210.2020.1706483>
- Cui, J., Li, F., & Shi, Z. L. (2019). Origin and evolution of pathogenic coronaviruses. *Nature Reviews Microbiology*, 17(3), 181-192. <https://doi.org/10.1038/s41579-018-0118-9>
- Douangamath, A., Fearon, D., Gehrtz, P., Krojer, T., Lukacik, P., Owen, C. D., Resnick, E., Strain-Damerell, C., Aimon, A., Abranyi-Balogh, P., Brandao-Neto, J., Carbery, A., Davison, G., Dias, A., Downes, T. D., Dunnett, L., Fairhead, M., Firth, J. D., Jones, S. P., Keeley, A., Keseru, G. M., Klein, H. F., Martin, M. P., Noble, M. E. M., O'Brien, P., Powell, A., Reddi, R. N., Skyner, R., Snee, M., Waring, M. J., Wild, C., London, N., von Delft, F., & Walsh, M. A. (2020). Crystallographic and electrophilic fragment screening of the SARS-CoV-2 main protease. *Nature Communications*, 11(1), 5047. <https://doi.org/10.1038/s41467-020-18709-w>
- Fowler Iii, A. A., Kim, C., Lepler, L., Malhotra, R., Debesa, O., Natarajan, R., Fisher, B. J., Syed, A., DeWilde, C., Priday, A., & Kasirajan, V. (2017). Intravenous vitamin C as adjunctive therapy for enterovirus/rhinovirus induced acute respiratory distress syndrome. *World J Crit Care Med*, 6(1), 85-90. <https://doi.org/10.5492/wjccm.v6.i1.85>
- Furuya, A., Uozaki, M., Yamasaki, H., Arakawa, T., Arita, M., & Koyama, A. H. (2008). Antiviral effects of ascorbic and dehydroascorbic acids in vitro. *Int J Mol Med*, 22(4), 541-545. <https://www.ncbi.nlm.nih.gov/pubmed/18813862>
- Gunther, S., Reinke, P. Y. A., Fernandez-Garcia, Y., Lieske, J., Lane, T. J., Ginn, H. M., Koua, F. H. M., Ehrt, C., Ewert, W., Oberthuer, D., Yefanov, O., Meier, S., Lorenzen, K., Krichel, B., Kopicki, J. D., Gelisio, L., Brehm, W., Dunkel, I., Seychell, B., Gieseler, H., Norton-Baker, B., Escudero-Perez, B., Domaracky, M., Saouane, S., Tolstikova, A., White, T. A., Hanle, A., Groessler, M., Fleckenstein, H., Trost, F., Galchenkova, M., Gevorkov, Y., Li, C., Awel, S., Peck, A., Barthelmess, M., Schlunzen, F., Lourdu Xavier, P., Werner, N., Andaleeb, H., Ullah, N., Falke, S., Srinivasan, V., Franca, B. A., Schwinzer, M., Brognaro, H., Rogers, C., Melo, D., Zaitseva-Doyle, J. J., Knoska, J., Pena-Murillo, G. E., Mashhour, A. R., Hennicke, V., Fischer, P., Hakanpaa, J., Meyer, J., Gribbon, P., Ellinger, B., Kuzikov, M., Wolf, M., Beccari, A. R., Bourenkov, G., von Stetten, D., Pompidor, G., Bento, I., Panneerselvam, S., Karpics, I., Schneider, T. R., Garcia-Alai, M. M., Niebling, S., Gunther, C., Schmidt, C., Schubert, R., Han, H., Boger, J., Monteiro, D. C. F., Zhang, L., Sun, X., Pletzer-Zelgert, J., Wollenhaupt, J., Feiler, C. G., Weiss, M. S., Schulz, E. C., Mehrabi, P., Karnicar, K., Usenik, A., Loboda, J., Tidow, H., Chari, A., Hilgenfeld, R., Uetrecht, C., Cox, R., Zaliani, A., Beck, T., Rarey, M., Gunther, S., Turk, D., Hinrichs, W., Chapman, H. N., Pearson, A. R., Betzel, C., &

- Meents, A. (2021). X-ray screening identifies active site and allosteric inhibitors of SARS-CoV-2 main protease. *Science*. <https://doi.org/10.1126/science.abf7945>
- Harakeh, S., Jariwalla, R. J., & Pauling, L. (1990). Suppression of Human-Immunodeficiency-Virus Replication by Ascorbate in Chronically and Acutely Infected-Cells. *Proc Natl Acad Sci U S A*, 87(18), 7245-7249. <https://doi.org/DOI 10.1073/pnas.87.18.7245>
- Hilgenfeld, R. (2014). From SARS to MERS: crystallographic studies on coronaviral proteases enable antiviral drug design. *Febs Journal*, 281(18), 4085-4096. <https://doi.org/10.1111/febs.12936>
- Hoog, S. S., Smith, W. W., Qiu, X., Janson, C. A., Hellmig, B., McQueney, M. S., O'Donnell, K., O'Shannessy, D., DiLella, A. G., Debouck, C., & Abdel-Meguid, S. S. (1997). Active site cavity of herpesvirus proteases revealed by the crystal structure of herpes simplex virus protease/inhibitor complex. *Biochemistry*, 36(46), 14023-14029. <https://doi.org/10.1021/bi9712697>
- Klein, M. (1945). The Mechanism of the Virucidal Action of Ascorbic Acid. *Science*, 101(2632), 587-589. <https://doi.org/10.1126/science.101.2632.587>
- Kneller, D. W., Galanie, S., Phillips, G., O'Neill, H. M., Coates, L., & Kovalevsky, A. (2020). Malleability of the SARS-CoV-2 3CL M(pro) Active-Site Cavity Facilitates Binding of Clinical Antivirals. *Structure*, 28(12), 1313-1320 e1313. <https://doi.org/10.1016/j.str.2020.10.007>
- Liebschner, D., Afonine, P. V., Moriarty, N. W., Poon, B. K., Sobolev, O. V., Terwilliger, T. C., & Adams, P. D. (2017). Polder maps: improving OMIT maps by excluding bulk solvent. *Acta Crystallogr D Struct Biol*, 73(Pt 2), 148-157. <https://doi.org/10.1107/S2059798316018210>
- Mescic Macan, A., Gazivoda Kraljevic, T., & Raic-Malic, S. (2019). Therapeutic Perspective of Vitamin C and Its Derivatives. *Antioxidants (Basel)*, 8(8). <https://doi.org/10.3390/antiox8080247>
- Minor, W., Cymborowski, M., Otwinowski, Z., & Chruszcz, M. (2006). HKL-3000: the integration of data reduction and structure solution - from diffraction images to an initial model in minutes. *Acta Crystallographica Section D-Structural Biology*, 62, 859-866. <Go to ISI>://WOS:000239119800003
- Murshudov, G. N., Skubak, P., Lebedev, A. A., Pannu, N. S., Steiner, R. A., Nicholls, R. A., Winn, M. D., Long, F., & Vagin, A. A. (2011). REFMAC5 for the refinement of macromolecular crystal structures. *Acta Crystallogr D Biol Crystallogr*, 67(Pt 4), 355-367. <https://doi.org/10.1107/S0907444911001314>
- Oeffner, R. D., Bunkoczi, G., McCoy, A. J., & Read, R. J. (2013). Improved estimates of coordinate error for molecular replacement. *Acta Crystallographica Section D-Biological Crystallography*, 69, 2209-2215. <https://doi.org/Doi 10.1107/S0907444913023512>
- Pauling, L. (1970). *Vitamin C and the Common Cold*. W. H. Freeman and Company.
- Ramajayam, R., Tan, K. P., & Liang, P. H. (2011). Recent development of 3C and 3CL protease inhibitors for anti-coronavirus and anti-picornavirus drug discovery. *Biochem Soc Trans*, 39(5), 1371-1375. <https://doi.org/10.1042/BST0391371>
- Sharma, A., & Gupta, S. P. (2017). Fundamentals of Viruses and Their Proteases. *Viral Proteases and Their Inhibitors*, 1-24. <https://doi.org/10.1016/B978-0-12-809712-0.00001-0>
- Thomas, S., Patel, D., Bittel, B., Wolski, K., Wang, Q., Kumar, A., Il'Giovine, Z. J., Mehra, R., McWilliams, C., Nissen, S. E., & Desai, M. Y. (2021). Effect of High-Dose Zinc and

- 311 Ascorbic Acid Supplementation vs Usual Care on Symptom Length and Reduction
- 312 Among Ambulatory Patients With SARS-CoV-2 Infection: The COVID A to Z
- 313 Randomized Clinical Trial. *JAMA Netw Open*, 4(2), e210369.
- 314 <https://doi.org/10.1001/jamanetworkopen.2021.0369>
- 315 Wu, F., Zhao, S., Yu, B., Chen, Y.-M., Wang, W., Song, Z.-G., Hu, Y., Tao, Z.-W., Tian, J.-H.,
- 316 Pei, Y.-Y., Yuan, M.-L., Zhang, Y.-L., Dai, F.-H., Liu, Y., Wang, Q.-M., Zheng, J.-J.,
- 317 Xu, L., Holmes, E. C., & Zhang, Y.-Z. (2020). A new coronavirus associated with human
- 318 respiratory disease in China. *Nature*, 579, 4.
- 319 <https://doi.org/https://doi.org/10.1038/s41586-020-2008-3>
- 320 Zhang, L. L., Lin, D. Z., Kusov, Y., Nian, Y., Ma, Q. J., Wang, J., von Brunn, A., Leyssen, P.,
- 321 Lanko, K., Neyts, J., de Wilde, A., Snijder, E. J., Liu, H., & Hilgenfeld, R. (2020). alpha-
- 322 Ketoamides as Broad-Spectrum Inhibitors of Coronavirus and Enterovirus Replication:
- 323 Structure-Based Design, Synthesis, and Activity Assessment. *Journal of Medicinal*
- 324 *Chemistry*, 63(9), 4562-4578. <Go to ISI>://WOS:000535279800012
- 325 Zhang, L. L., Lin, D. Z., Sun, X. Y. Y., Curth, U., Drosten, C., Sauerhering, L., Becker, S., Rox,
- 326 K., & Hilgenfeld, R. (2020). Crystal structure of SARS-CoV-2 main protease provides a
- 327 basis for design of improved alpha-ketoamide inhibitors. *Science*, 368(6489), 409-+. <Go
- 328 to ISI>://WOS:000528513300041
- 329 Zhao, B., Ling, Y., Li, J., Peng, Y. B., Huang, J., Wang, Y. H., Qu, H. P., Gao, Y., Li, Y. C., Hu,
- 330 B. J., Lu, S. H., Lu, H. Z., Zhang, W. H., & Mao, E. Q. (2021). Beneficial aspects of high
- 331 dose intravenous vitamin C on patients with COVID-19 pneumonia in severe condition: a
- 332 retrospective case series study. *Annals of Palliative Medicine*, 10(2), 1599-+.
- 333 <https://doi.org/10.21037/apm-20-1387>
- 334